

Shear Viscosity in the $O(N)$ Model

Gert Aarts* and J. M. Martínez Resco[†]

*Department of Physics, The Ohio State University
174 West 18th Avenue, Columbus, OH 43210, USA*

February 18, 2004

Abstract

We compute the shear viscosity in the $O(N)$ model at first nontrivial order in the large N expansion. The calculation is organized using the $1/N$ expansion of the 2PI effective action (2PI- $1/N$ expansion) to next-to-leading order, which leads to an integral equation summing ladder and bubble diagrams. We also consider the weakly coupled theory for arbitrary N , using the three-loop expansion of the 2PI effective action. In the limit of weak coupling and vanishing mass, we find an approximate analytical solution of the integral equation. For general coupling and mass, the integral equation is solved numerically using a variational approach. The shear viscosity turns out to be close to the result obtained in the weak-coupling analysis.

*email: aarts@mps.ohio-state.edu

[†]email: marej@mps.ohio-state.edu

1 Introduction

Due to the recent progress in relativistic heavy ion collisions and cosmology, detailed theoretical investigations of the dynamics of quantum fields out of equilibrium have become an active subject of research. A successful approach to solve the dynamics of quantum fields far from equilibrium as well as the subsequent stage of equilibration and thermalization makes use of the so-called two-particle-irreducible (2PI) effective action (see Refs. [1]-[13] for recent nonequilibrium applications).

The final stages of thermalization in systems out of equilibrium with conserved quantities can be described by hydrodynamics, characterized by an equation of state and transport coefficients. Recently, we investigated the connection between the 2PI effective action and transport coefficients for a variety of field theories and found that the lowest nontrivial truncation of the 2PI effective action determines correctly transport coefficients in a weak coupling or $1/N$ expansion at leading (logarithmic) order [14].¹ We emphasized that this result provides an important benchmark to validate commonly used truncation schemes for nonequilibrium quantum field dynamics.²

In applications to heavy ion dynamics, successful hydrodynamical descriptions of heavy ion collisions are so far based on ideal hydrodynamics, assuming infinitely fast thermalization and vanishing transport coefficients [17]. The extension to nonideal hydrodynamics is nontrivial, but the effects of viscous corrections are currently under investigation [18]. In order to make further progress, it is crucial to know the magnitude of transport coefficients quantitatively [18].

Transport coefficients in relativistic plasmas at high temperature can be computed following different approaches. The first complete calculations in hot gauge theories were done using kinetic theory: to leading logarithmic order in the weak coupling expansion [19], to full leading order [20, 21], and in the large N_f limit [22]. Using field theory techniques, the shear and bulk viscosities were obtained in a single-component scalar field theory with cubic and quartic interactions through the summation of an infinite series of ladder diagrams [23] (for a more concise analysis of the shear viscosity, see [24]). In Ref. [25] a simple and economical way was presented to carry out the sum of ladder diagrams contributing to the shear viscosity to leading order in a quartic scalar theory and to the shear viscosity and electrical conductivity in the leading-log approximation in (non)abelian gauge theories. The Ward identity in the calculation of the electrical conductivity in QED was studied in Ref. [26], while an alternative diagrammatic approach employing a dynamical renormalization group

¹For the bulk viscosity it is necessary to go to higher-order truncations [15].

²In this context it would be interesting to compute transport coefficients within the so-called 2PPI effective action approach [16].

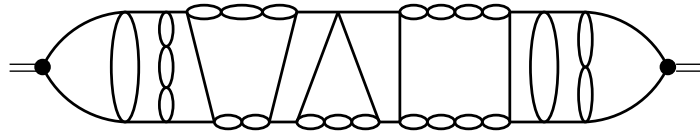


Figure 1: Typical skeleton diagram that contributes to the shear viscosity in the $O(N)$ model at first nontrivial order in the large N limit. The black dots with tiny lines represent the external bilinear operators.

to study the conductivity was presented in Ref. [27]. The prospects of extracting transport coefficients nonperturbatively using lattice QCD have been discussed in Ref. [28] and first results have been obtained [29] (see also [30]). In strongly coupled supersymmetric Yang-Mills theories, the shear viscosity has been computed with the help of the AdS/CFT correspondence [31]. Finally, the shear viscosity has been computed in the hadronic phase using phenomenological models [32, 33].

In this paper we consider the $O(N)$ model in its symmetric phase and compute the shear viscosity to first nontrivial order in the $1/N$ expansion. The $O(N)$ model is widely used when applying methods and techniques in thermal and nonequilibrium field theory, because without running into the issue of gauge invariance, it still leaves a nontrivial problem to solve. Moreover, it acts as a low energy effective description of QCD (for $N = 4$) and is frequently used in early cosmology (inflation, reheating). The large N expansion offers the possibility to explore the behavior of transport coefficients outside the weak-coupling domain and in combination with the 2PI effective action, it naturally leads to the inclusion of the required medium effects in the single particle propagators. We use a field theory approach to compute the shear viscosity. As we will show below, a typical ladder diagram that contributes at leading order is shown in Fig. 1. We note that the lines in this diagram are dressed propagators, so it should be regarded as a skeleton diagram. As we have recently shown [14], the summation of these classes of diagrams is neatly organized using the 2PI effective action. In particular, the 2PI- $1/N$ expansion to next-to-leading order (NLO) [4, 6] sums precisely the relevant set of diagrams.

The paper is organized as follows. In Section 2 we describe the 2PI effective action for the $O(N)$ model and write down the ensuing integral equation at next-to-leading order in the $1/N$ expansion. We argue that it sums all necessary diagrams that contribute to the shear viscosity at leading order. In the next Section we study the various elements that appear in the integral equation and which are essential for its calculation: the single particle spectral function, the gap equation for the mass and its renormalization, the auxiliary correlator summing the chain of bubbles diagrams, and

the thermal width. In Section 4 we derive a compact expression for the shear viscosity in terms of an effective vertex summing the ladder diagrams. Section 5 is devoted to the integral equation for the effective vertex. We show how to cast the problem of solving it into a variational one, better suited for numerical analysis. In Section 6 we study the weak-coupling limit of the integral equation and find an analytical result in the limit of ultrahard momentum. In Section 7 we solve numerically the variational problem and present the results for the shear viscosity. The final Section is devoted to the conclusions. In Appendix A we consider the weakly coupled $O(N)$ model for arbitrary N using the three-loop expansion of the 2PI effective action.

2 2PI- $1/N$ expansion

We consider a real scalar N -component quantum field ϕ_a ($a = 1, \dots, N$) with a classical $O(N)$ -invariant action,

$$S[\phi] = \int_x \left[\frac{1}{2} \partial_0 \phi_a \partial_0 \phi_a - \frac{1}{2} \partial_i \phi_a \partial_i \phi_a - \frac{1}{2} m_0^2 \phi_a \phi_a - \frac{\lambda_0}{4!N} (\phi_a \phi_a)^2 \right]. \quad (1)$$

The mass parameter m_0 and coupling constant λ_0 are bare parameters. To the order we are working, field renormalization is not necessary. We use the notation

$$\int_x = \int_{\mathcal{C}} dx^0 \int d^3x, \quad (2)$$

where \mathcal{C} is a contour in the complex-time plane. We will work in the imaginary time formalism, so below we specialize to the Matsubara contour, running from 0 to $-i/T$.

According to the Kubo formula, the shear viscosity can be obtained from the slope of a spectral function at zero frequency,

$$\eta = \frac{1}{20} \frac{\partial}{\partial q^0} \rho_{\pi\pi}(q^0, \mathbf{0}) \Big|_{q^0=0}, \quad (3)$$

where

$$\rho_{\pi\pi}(x - y) = \langle [\pi_{ij}(x), \pi_{ij}(y)] \rangle, \quad (4)$$

with π_{ij} the traceless part of the spatial energy-momentum tensor,

$$\pi_{ij}(x) = \partial_i \phi_a(x) \partial_j \phi_a(x) - \frac{1}{3} \delta_{ij} \partial_k \phi_a(x) \partial_k \phi_a(x). \quad (5)$$

It is well known from weak coupling studies that a one loop calculation of the shear viscosity is incorrect, since diagrams that appear at higher order in the loop

expansion contribute at leading order and the computation must be carried out using dressed propagators [23, 25]. For a single-component scalar field ($N = 1$), Jeon showed that these higher order diagrams are ladder diagrams, where the rung in the ladder is a single bubble [23]. Due to the kinematical configuration, the propagators on the side rails suffer from pinching poles. As a result the thermal width, which is determined by the imaginary part of the self energy, has to be included in these propagators, while the real part is subleading and can be neglected (at weak coupling). The picture is quite similar for gauge theories at leading logarithmic order in the weak coupling limit [25, 26]. The ladder series is conveniently summed through an integral equation for an effective vertex [23, 24, 25]. We have shown recently that this integral equation in the required kinematic configuration appears naturally in the 2PI effective action formalism [14]. In the $1/N$ expansion, in which we are interested here, the presence of pinching poles also leads to higher order diagrams in the loop expansion contributing at leading order, and the 2PI effective action formalism neatly organizes this calculation as well, as we describe now.

The 2PI effective action is a functional of the time-ordered two-point function $G_{ab}(x, y) = \langle T_c \phi_a(x) \phi_b(y) \rangle$ and can be parametrized as [34, 35]

$$\Gamma[G] = \frac{i}{2} \text{Tr} \ln G^{-1} + \frac{i}{2} \text{Tr} G_0^{-1} (G - G_0) + \Gamma_2[G]. \quad (6)$$

Throughout we consider $\langle \phi_a(x) \rangle = 0$. The classical inverse propagator iG_0^{-1} is given by

$$iG_{0,ab}^{-1}(x, y) = -[\square_x + m_0^2] \delta_{ab} \delta_C(x - y), \quad (7)$$

with $\delta_C(x - y) \equiv \delta_C(x^0 - y^0) \delta(\mathbf{x} - \mathbf{y})$. $\Gamma_2[G]$ is the sum of all 2-particle irreducible (2PI) diagrams with no external legs and exact propagators on the internal lines. Extremizing this effective action,

$$\frac{\delta \Gamma[G]}{\delta G_{ab}(x, y)} = 0, \quad (8)$$

leads to a Dyson equation for the two-point function

$$G_{ab}^{-1}(x, y) = G_{0,ab}^{-1}(x, y) - \Sigma_{ab}(x, y) \quad (9)$$

where the self energy

$$\Sigma_{ab}(x, y) \equiv 2i \frac{\delta \Gamma_2[G]}{\delta G_{ab}(x, y)} \quad (10)$$

depends on the full propagator G .

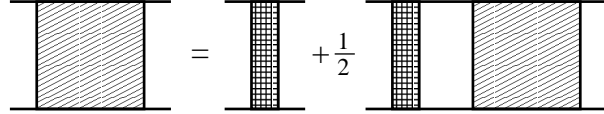


Figure 2: Integral equation for the 4-point function.

Within the 2PI formalism, a 4-point vertex function $\Gamma^{(4)}$ appears, defined as the usual connected 4-point function with the external legs removed. This 4-point function obeys an integral equation that can be obtained using standard functional relations [34] (see Fig. 2)

$$\begin{aligned} \Gamma_{ab;cd}^{(4)}(x, y; x', y') &= \Lambda_{ab;cd}(x, y; x', y') \\ &+ \frac{1}{2} \int_{ww'zz'} \Lambda_{ab;ef}(x, y; w, z) G_{ee'}(w, w') G_{ff'}(z, z') \Gamma_{e'f';cd}^{(4)}(w', z'; x', y'). \end{aligned} \quad (11)$$

The kernel or rung Λ is defined as

$$\Lambda_{ab;cd}(x, y; x', y') = 2 \frac{\delta \Sigma_{ab}(x, y)}{\delta G_{cd}(x', y')}. \quad (12)$$

Semicolons separate indices with a different origin [14].

The relations so far are general. We now specialize to the 2PI- $1/N$ expansion to NLO. The 2PI part of the effective action can be written as [4, 6]

$$\Gamma_2[G] = \Gamma_2^{\text{LO}}[G] + \Gamma_2^{\text{NLO}}[G] + \dots, \quad (13)$$

where (see Fig. 3)

$$\Gamma_2^{\text{LO}}[G] = -\frac{\lambda_0}{4!N} \int_x G_{aa}(x, x) G_{bb}(x, x), \quad (14)$$

$$\Gamma_2^{\text{NLO}}[G] = \frac{i}{2} \text{Tr} \ln \mathbf{B}, \quad (15)$$

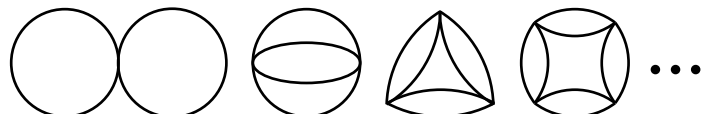


Figure 3: Contributions to the 2PI effective action in the $O(N)$ model in the 2PI- $1/N$ expansion at LO and NLO. Only the first few diagrams at NLO are shown.

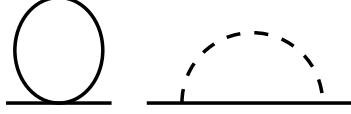


Figure 4: Contributions to the self energy at LO and NLO. The auxiliary correlator D is represented by the dashed line.

$$\rangle \cdots \langle = \times + \circ \cdots \langle$$

Figure 5: Integral equation for the auxiliary correlator D .

with

$$\mathbf{B}(x, y) = \delta_C(x - y) - \frac{i\lambda_0}{3N} \Pi(x, y). \quad (16)$$

The function \mathbf{B} depends on the single bubble diagram defined by

$$\Pi(x, y) = -\frac{1}{2} G_{ab}(x, y) G_{ab}(x, y). \quad (17)$$

Expanding the logarithm in Eq. (15) generates the closed chain of bubble diagrams as in Fig. 3. The self energy follows from Eq. (10). We write $\Sigma = \Sigma^{\text{LO}} + \Sigma^{\text{NLO}}$, with

$$\Sigma_{ab}^{\text{LO}}(x, y) = -i \frac{\lambda_0}{6N} \delta_{ab} G_{cc}(x, x) \delta_C(x - y), \quad (18)$$

$$\Sigma_{ab}^{\text{NLO}}(x, y) = -G_{ab}(x, y) D(x, y), \quad (19)$$

shown in Fig. 4. Here we introduced the auxiliary correlator

$$D(x, y) = \frac{i\lambda_0}{3N} \mathbf{B}^{-1}(x, y). \quad (20)$$

From the identity $\mathbf{B}^{-1} \mathbf{B} = 1$ it follows that the auxiliary correlator obeys

$$D(x, y) = \frac{i\lambda_0}{3N} \left[\delta_C(x - y) + \int_z \Pi(x, z) D(z, y) \right], \quad (21)$$

which is depicted in Fig. 5. For the rung, we write $\Lambda = \Lambda^{\text{LO}} + \Lambda^{\text{NLO}}$, and find (see Fig. 6)

$$\Lambda_{ab;cd}^{\text{LO}}(x, y; x', y') = -\frac{i\lambda_0}{3N} \delta_{ab} \delta_{cd} \delta_C(x - y) \delta_C(x - y') \delta_C(x' - y), \quad (22)$$

$$\begin{aligned} \Lambda_{ab;cd}^{\text{NLO}}(x, y; x', y') = & -[\delta_{ac} \delta_{bd} + \delta_{ad} \delta_{bc}] D(x, y) \delta_C(x - x') \delta_C(y - y') \\ & + 2G_{ab}(x, y) D(x, x') D(y, y') G_{cd}(x', y'). \end{aligned} \quad (23)$$

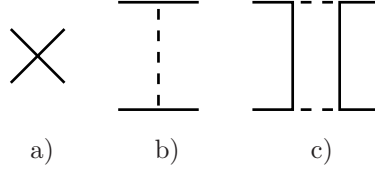


Figure 6: 4-point kernel in the 2PI- $1/N$ expansion of the $O(N)$ model at LO and NLO.

Finally, we specialize to the $O(N)$ -symmetric case, take $G_{ab}(x, y) = \delta_{ab}G(x, y)$ and $\Sigma_{ab}(x, y) = \delta_{ab}\Sigma(x, y)$, choose the Matsubara contour and write the equations in momentum space. The final set of equations then reads

$$G(P) = \frac{1}{\omega_n^2 + \mathbf{p}^2 + m_0^2 + \Sigma(P)}, \quad (24)$$

with

$$\Sigma^{\text{LO}}(P) = \frac{\lambda_0}{6} \oint_K G(K), \quad (25)$$

$$\Sigma^{\text{NLO}}(P) = - \oint_K G(P + K)D(K), \quad (26)$$

and

$$D(P) = \frac{1}{-3N/\lambda_0 + \Pi(P)}, \quad (27)$$

$$\Pi(P) = -\frac{N}{2} \oint_K G(P + K)G(K). \quad (28)$$

The 4-point function obeys

$$\Gamma_{ab;cd}^{(4)}(R, K) = \Lambda_{ab;cd}(R, K) + \frac{1}{2} \oint_P \Lambda_{ab;ef}(R, P)G^2(P)\Gamma_{ef;cd}^{(4)}(P, K), \quad (29)$$

with the kernel

$$\Lambda_{ab;cd}^{\text{LO}}(R, P) = -\frac{\lambda_0}{3N}\delta_{ab}\delta_{cd}, \quad (30)$$

$$\begin{aligned} \Lambda_{ab;cd}^{\text{NLO}}(R, P) = & [\delta_{ac}\delta_{bd} + \delta_{ad}\delta_{bc}] D(R - P) \\ & + 2\delta_{ab}\delta_{cd} \oint_L G(R - L)D^2(L)G(L - P). \end{aligned} \quad (31)$$

Here we used the notation $P = (i\omega_n, \mathbf{p})$, where $\omega_n = 2\pi nT$ ($n \in \mathbb{Z}$) is the Matsubara frequency, and

$$\oint_K = T \sum_n \int_{\mathbf{k}}, \quad \int_{\mathbf{k}} = \int \frac{d^3 k}{(2\pi)^3}. \quad (32)$$

In the remainder of this section, we argue that the set of Eqs. (24)-(31) sum all the diagrams contributing to the shear viscosity at leading order in the $1/N$ expansion. First we note that the one loop contribution to the viscosity is proportional to N^2 . Here, one factor of N arises from the group indices running in the loop, the other originates from the pair of pinching poles in the loop. Pinching poles are screened by the imaginary part of the retarded self energy Σ , which appears first at NLO (the leading order contribution to Σ is real). Since pinching poles are sensitive to the inverse of the imaginary part, each pair of pinching poles gives a contribution that scales as N . Therefore the shear viscosity takes the form³

$$\eta = N^2 T^3 \left[F \left(\lambda(\mu), \frac{m_R}{T}, \frac{\mu}{T} \right) + \mathcal{O} \left(\frac{1}{N} \right) \right], \quad (33)$$

where m_R is the renormalized mass in vacuum and $\lambda(\mu)$ is the renormalized coupling constant at the scale μ . The shear viscosity is independent of μ . It is now straightforward to identify which diagrams contribute to the shear viscosity at leading order. The auxiliary correlator D is proportional to $1/N$, see Eqs. (27, 28). Starting from the naive one-loop expression, adding a vertical D correlator as in Fig. 6b yields one extra pair of pinching poles that cancels the explicit $1/N$ from the D correlator. Therefore all vertical line insertions contribute at the same order. An insertion of the box rung (see Fig. 6c) results in two additional D correlators, one additional pair of pinching poles, and one additional closed loop over the group indices. Therefore also all box rung insertions contribute at the same order. Finally, the lowest order rung (see Fig. 6a), which would generate a string of bubbles, does not contribute to the shear viscosity. This was shown by Jeon [23] for the weakly coupled single component case and will be confirmed below. Rungs that are down by $1/N$ have additional D correlators but no compensating additional pinching poles or closed loops. Some examples of subleading rungs are shown in Fig. 7. We find therefore that the typical diagram contributing at leading order is as shown in Fig. 1. Throughout the paper we neglect subleading powers of N as indicated in Eq. (33).

Before analyzing the integral equation, which sums the required contributions, several elements are needed in detail. We study those in the next section.

³Note that the ratio of the shear viscosity and the entropy density s is proportional to N , and therefore always far above the lower bound conjectured recently, $\eta/s \geq 1/4\pi$ [36].

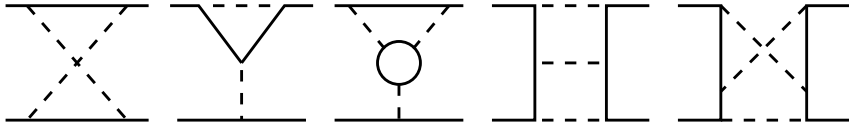


Figure 7: Examples of rungs that may contribute at next-to-leading order to the shear viscosity in the $1/N$ expansion.

3 Quasiparticles

In this section we study the single particle propagators that are dressed to account for plasma effects, which are crucial to the calculation of transport coefficients. A convenient way to study these effects is through the use of the single particle spectral density.

Analytically continuing the euclidean propagator (24) to real frequencies yields the retarded and advanced propagators,

$$\begin{aligned} G_R(P) &= G(i\omega_n \rightarrow p^0 + i0, \mathbf{p}) = G_A^*(P) \\ &= \frac{1}{-p_0^2 + \mathbf{p}^2 + m_0^2 + \text{Re}\Sigma_R(P) + i\text{Im}\Sigma_R(P)}, \end{aligned} \quad (34)$$

from which the spectral function is obtained as

$$\begin{aligned} \rho(P) &= -i [G_R(P) - G_A(P)] \\ &= \frac{-2\text{Im}\Sigma_R(P)}{[p_0^2 - \mathbf{p}^2 - m_0^2 - \text{Re}\Sigma_R(P)]^2 + [\text{Im}\Sigma_R(P)]^2}. \end{aligned} \quad (35)$$

The leading part of the self energy Σ^{LO} is of the same order as the mass in the $1/N$ expansion and hence it cannot be neglected. The real part of Σ_R^{NLO} on the other hand can be dropped since it is suppressed by $1/N$ compared to the leading piece.⁴ Since $\text{Im}\Sigma_R$ is proportional to $1/N$, the spectral density generically has a simple on-shell form in the large N limit,

$$\rho(P) = 2\pi \text{sgn}(p^0) \delta(p_0^2 - \omega_{\mathbf{p}}^2) + \mathcal{O}(1/N), \quad (36)$$

with

$$\omega_{\mathbf{p}} = \sqrt{\mathbf{p}^2 + M^2}, \quad M^2 = m_0^2 + \Sigma^{\text{LO}}. \quad (37)$$

However, when pairs of propagators with pinching poles are present, the imaginary part cannot be neglected as it separates the poles in the complex-energy plane that

⁴This is the reason wave function renormalization does not enter in this problem.

approach the real axis from below and above [23, 25]. In this case, the full propagator $G(P)$ has a cut along the whole real p^0 axis since $\text{Im}\Sigma_R(P)$ is nonvanishing for all real p^0 . Moreover, the product of retarded and advanced propagators is directly proportional to its inverse,

$$G_R(P)G_A(P) = \frac{1}{[p_0^2 - \mathbf{p}^2 - m_0^2 - \text{Re}\Sigma_R(P)]^2 + [\text{Im}\Sigma_R(P)]^2} = \frac{\rho(P)}{-2\text{Im}\Sigma_R(P)}. \quad (38)$$

In the limit of large N we may use Eq. (36) and this expression reduces to

$$G_R(P)G_A(P) = \frac{\rho(P)}{2p^0\Gamma_{\mathbf{p}}} + \mathcal{O}(1), \quad (39)$$

with $\Gamma_{\mathbf{p}}$ the (on-shell) thermal width defined from the imaginary part of the retarded self energy as

$$\Gamma_{\mathbf{p}} = -\frac{\text{Im}\Sigma_R(P)}{p^0} \Big|_{p^0=\pm\omega_{\mathbf{p}}}. \quad (40)$$

In the remainder of this section we study the corrections introduced by the self energy. The real part of Σ leads to a gap equation for the mass which requires renormalization of both the mass parameter and coupling constant. The imaginary part is computed in terms of the auxiliary correlator D , which we work out in detail.

3.1 Gap equation and renormalization

Since the real part of Σ_R^{NLO} can be systematically neglected, the gap equation for the mass parameter M reads

$$M^2 = m_0^2 + \frac{\lambda_0}{6} \oint_P G(P), \quad (41)$$

with

$$G(P) = \frac{1}{\omega_n^2 + \mathbf{p}^2 + M^2}. \quad (42)$$

This gap equation is divergent and in order to renormalize it⁵ we also need the integral equation for the 4-point function, Eq. (29), at lowest order. In this approximation the 4-point function is momentum independent and Eq. (29) can be solved as

$$\Gamma_{ab;cd}^{(4)}(R, K) = \delta_{ab}\delta_{cd}\Gamma^{(4)}, \quad \frac{1}{\Gamma^{(4)}} = -\frac{3N}{\lambda_0} + \Pi(0), \quad (43)$$

⁵See Refs. [37, 38] for recent studies of renormalization in the 2PI effective action formalism.

with the single bubble at zero momentum

$$\Pi(0) = -\frac{N}{2} \oint_P G^2(P). \quad (44)$$

We note that the equation for the 4-point function is identical to the equation for the auxiliary correlator $D(P)$ at zero momentum. Therefore the renormalization carried out to obtain a finite gap equation renders $D(P)$ finite too.

In order to regulate the divergent integrals we use dimensional regularization in $3-2\epsilon$ dimensions. Both λ_0 and $\Gamma^{(4)}$ have dimension $\mu^{2\epsilon}$. We introduce a dimensionless coupling λ_R via

$$\Gamma^{(4)} = -\frac{\lambda_R \mu^{2\epsilon}}{3N}, \quad (45)$$

such that the equations to renormalize read

$$\frac{1}{\lambda_R} = \frac{\mu^{2\epsilon}}{\lambda_0} + \frac{\mu^{2\epsilon}}{6} \oint_P G^2(P), \quad (46)$$

$$M^2 = m_0^2 + \frac{\lambda_0}{6} \oint_P G(P). \quad (47)$$

Since renormalization can be carried out at zero temperature, we only compute the bubble in the vacuum

$$\frac{1}{\lambda_R} = \frac{\mu^{2\epsilon}}{\lambda_0} + \frac{1}{96\pi^2} \left(\frac{1}{\epsilon} + \ln(4\pi) - \gamma_E + 2 \ln \frac{\mu}{m_R} \right), \quad (48)$$

where m_R is the renormalized mass at zero temperature. Introducing the running coupling constant in the \overline{MS} scheme $\lambda(\mu)$ via

$$\frac{1}{\lambda(\mu)} \equiv \frac{\mu^{2\epsilon}}{\lambda_0} + \frac{1}{96\pi^2} \left(\frac{1}{\epsilon} + \ln(4\pi) - \gamma_E \right), \quad (49)$$

we find

$$\frac{1}{\lambda_R} = \frac{1}{\lambda(\mu)} + \frac{1}{48\pi^2} \ln \frac{\mu}{m_R}. \quad (50)$$

The running coupling $\lambda(\mu)$ obeys the usual renormalization group (RG) equation with the correct β function for the $O(N)$ model in the large N limit, $\beta(\lambda) = \lambda^2/(48\pi^2)$.

Returning to the gap equation (47) at zero temperature, we find

$$m_R^2 = m_0^2 - \frac{\lambda_0 \mu^{-2\epsilon}}{6} \frac{m_R^2}{16\pi^2} \left[\frac{1}{\epsilon} + \ln(4\pi) - \gamma_E + 1 + 2 \ln \frac{\mu}{m_R} \right], \quad (51)$$

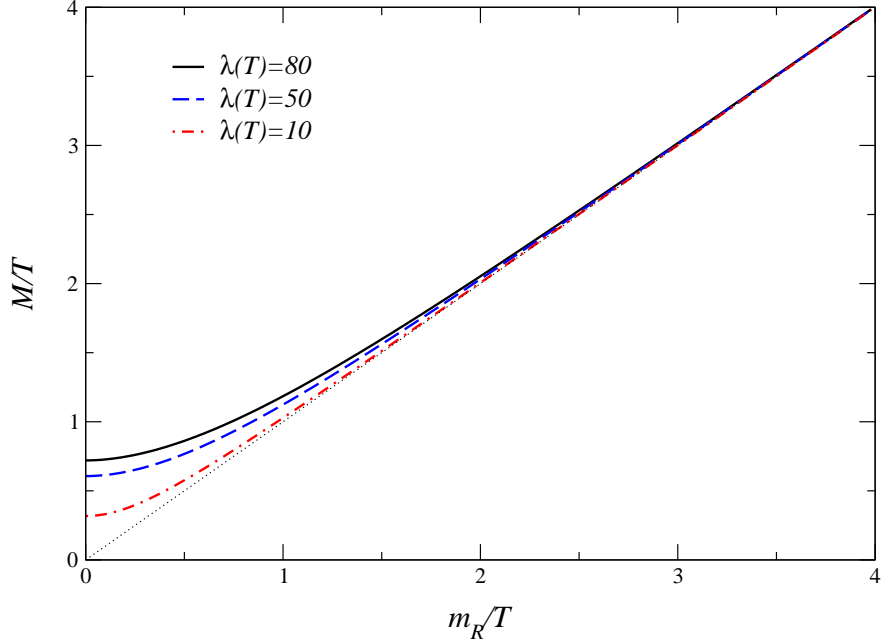


Figure 8: Finite temperature mass M/T as a function of the renormalized mass at zero temperature m_R/T for 3 different values of $\lambda(T)$.

Combining Eqs. (47, 49, 51), we arrive at the renormalized gap equation at finite temperature

$$M^2 = m_R^2 - \frac{\lambda(\mu)}{96\pi^2} \left[(M^2 - m_R^2) \left(1 + \ln \frac{\mu^2}{m_R^2} \right) + M^2 \ln \frac{m_R^2}{M^2} \right] + \frac{\lambda(\mu)}{6} \int_{\mathbf{p}} \frac{n(\omega_{\mathbf{p}})}{\omega_{\mathbf{p}}}, \quad (52)$$

where $n(\omega) = 1/(e^{\omega/T} - 1)$ is the Bose distribution function. The solution of this gap equation is independent of the renormalization scale μ . A numerical solution of the gap equation for three values of $\lambda(\mu = T)$ is shown in Fig. 8.

There is one additional issue related to renormalization that needs to be considered. This scalar theory has a Landau pole at the scale $\Lambda_L = \mu e^{48\pi^2/\lambda(\mu)}$, where the running coupling constant diverges. One has to require that all physical energy scales involved in the problem, i.e. m_R , M , and T , are much smaller than the one associated with the Landau pole. This imposes a restriction on which values of $\lambda(\mu)$ and m_R can be considered. Taking, for example, T to be the largest scale and demanding that $\Lambda_L/T \gtrsim 40$, we find that $\lambda(\mu = T) \lesssim 48\pi^2/\ln 40 \approx 128$.

3.2 Auxiliary correlator

Before proceeding with a calculation of the thermal width, we need to consider the chain of bubbles summed by the auxiliary correlator D . The single bubble is given by

$$\Pi(P) = -\frac{N}{2} \sum_K G(P+K)G(K), \quad (53)$$

which after performing the Matsubara sum reads

$$\begin{aligned} \Pi(P) = -\frac{N}{2} \int_{\mathbf{k}} \frac{1}{4\omega_{\mathbf{k}}\omega_{\mathbf{r}}} & \left\{ [n(\omega_{\mathbf{r}}) - n(\omega_{\mathbf{k}})] \left(\frac{1}{i\omega_n + \omega_{\mathbf{k}} - \omega_{\mathbf{r}}} - \frac{1}{i\omega_n - \omega_{\mathbf{k}} + \omega_{\mathbf{r}}} \right) \right. \\ & \left. + [1 + n(\omega_{\mathbf{k}}) + n(\omega_{\mathbf{r}})] \left(\frac{1}{i\omega_n + \omega_{\mathbf{k}} + \omega_{\mathbf{r}}} - \frac{1}{i\omega_n - \omega_{\mathbf{k}} - \omega_{\mathbf{r}}} \right) \right\}, \end{aligned} \quad (54)$$

where $\mathbf{r} = \mathbf{k} + \mathbf{p}$. In order to separate the logarithmic divergence in the zero-temperature contribution we write

$$\Pi(P) = \Pi_0(P) + \Pi_T(P), \quad \Pi_0(P) = \Pi_0(0) + \Pi'_0(P), \quad (55)$$

where $\Pi_0(P)$ is the part without distribution functions. The divergent contribution $\Pi_0(0)$ is similar to the one computed for the renormalization of the coupling constant,

$$\Pi_0(0) = -\frac{N}{32\pi^2} \left(\frac{1}{\epsilon} + \ln 4\pi - \gamma_E + 2 \ln \frac{\mu}{M} \right), \quad (56)$$

while the remainder is finite and can be evaluated as

$$\Pi'_0(P) = -\frac{N}{16\pi^2} \left(1 + \frac{1}{2} \sqrt{1 + 4M^2/P^2} \ln \frac{\sqrt{1 + 4M^2/P^2} - 1}{\sqrt{1 + 4M^2/P^2} + 1} \right), \quad (57)$$

with $P^2 = \omega_n^2 + \mathbf{p}^2$. The easiest way to arrive at the above result is to go back to the original four-dimensional euclidean integral.

We are interested in the retarded bubble, obtained by analytical continuation $i\omega_n \rightarrow p^0 + i0$. For the finite contribution to the real part we write

$$\text{Re}\Pi_R^f(P) = \text{Re}\Pi_0'^R(P) + \text{Re}\Pi_T^R(P), \quad (58)$$

with

$$\begin{aligned} \text{Re}\Pi_0'^R(P) = -\frac{N}{16\pi^2} & \left\{ 1 + \frac{1}{2} [\Theta(s - 4M^2) + \Theta(-s)] \beta(P) \ln \left| \frac{1 - \beta(P)}{1 + \beta(P)} \right| \right. \\ & \left. - \Theta(4M^2 - s) \Theta(s) B(P) \arctan \frac{1}{B(P)} \right\}, \end{aligned} \quad (59)$$

where $s = p_0^2 - p^2$, and

$$\beta(P) = \sqrt{1 - \frac{4M^2}{p_0^2 - p^2}}, \quad B(P) = \sqrt{\frac{4M^2}{p_0^2 - p^2} - 1}, \quad (60)$$

and

$$\text{Re}\Pi_T^R(P) = -\frac{N}{16\pi^2 p} \int_0^\infty dk \frac{k}{\omega_{\mathbf{k}}} n(\omega_{\mathbf{k}}) \ln \left| \frac{(k+p_+)(k+p_-)}{(k-p_+)(k-p_-)} \right|, \quad (61)$$

with $p_\pm = \frac{1}{2} [p \pm p^0 \beta(P)]$. The remaining integral can be done numerically.

The imaginary part can be written in terms of single particle spectral functions as

$$\text{Im}\Pi_R(P) = -\frac{N}{4} \int_K \rho(P+K) \rho(K) [n(k^0) - n(p^0 + k^0)], \quad (62)$$

where

$$\int_K = \int \frac{d^4 k}{(2\pi)^4}, \quad (63)$$

and can be evaluated completely

$$\begin{aligned} \text{Im}\Pi_R(P) = & -\Theta(s - 4M^2) \frac{N}{32\pi} \left[\beta(P) + \frac{2T}{p} \ln \frac{1 - e^{-\bar{p}_+/T}}{1 - e^{-\bar{p}_-/T}} \right] \\ & -\Theta(-s) \frac{NT}{16\pi p} \ln \frac{1 - e^{-\bar{p}_+/T}}{1 - e^{\bar{p}_-/T}}, \end{aligned} \quad (64)$$

with $\bar{p}_\pm = \frac{1}{2} [p^0 \pm p\beta(P)]$.

The chain of bubbles is summed by the auxiliary correlator D in Eq. (27). The divergent piece of the single bubble $\Pi_0(0)$ is absorbed by coupling constant renormalization. The renormalized expression for D^{-1} reads

$$D^{-1}(P) = -3N \left[\frac{1}{\lambda(\mu)} - \frac{1}{96\pi^2} \ln \frac{M^2}{\mu^2} \right] + \Pi'_0(P) + \Pi_T(P). \quad (65)$$

The auxiliary correlator is renormalization group invariant. Retarded auxiliary propagators are obtained as $D_R(P) = D(i\omega_n \rightarrow p^0 + i0, \mathbf{p}) = D_A^*(P)$. The spectral density is

$$\rho_D(P) = -i [D_R(P) - D_A(P)] = \frac{-2\text{Im}\Pi_R(P)}{\left[3N/\lambda(M) - \text{Re}\Pi_R^f(P) \right]^2 + [\text{Im}\Pi_R(P)]^2}, \quad (66)$$

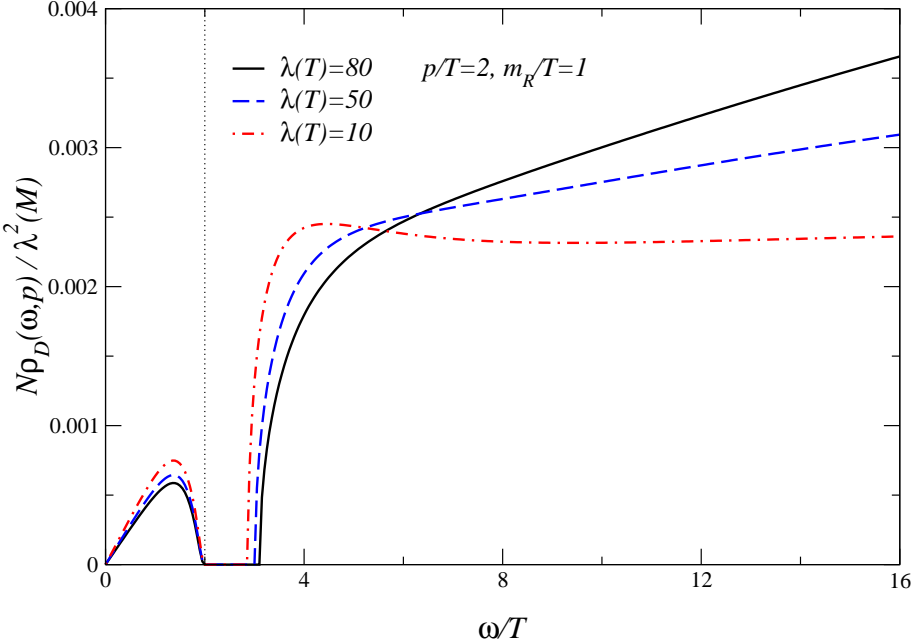


Figure 9: Spectral density $N\rho_D(\omega, \mathbf{p})/\lambda^2(M)$ as a function of ω/T for fixed $p/T = 2$, $m_R/T = 1$ and three values of the coupling $\lambda(\mu = T)$. The vertical line indicates the lightcone.

in terms of the RG invariant coupling

$$\frac{1}{\lambda(M)} = \frac{1}{\lambda(\mu)} - \frac{1}{96\pi^2} \ln \frac{M^2}{\mu^2}. \quad (67)$$

The spectral function is shown in Fig. 9 for a typical choice of parameters. We scaled out the trivial $N/\lambda^2(M)$ dependence. $\text{Im}\Pi_R(\omega, \mathbf{p})$ and therefore $\rho_D(\omega, \mathbf{p})$ are nonzero below the lightcone ($\omega^2 < p^2$) and above threshold ($\omega^2 > p^2 + 4M^2$). We note that for larger coupling constant the contribution below the lightcone diminishes. Fixing m_R and increasing $\lambda(T)$ results in a larger value for M (see Fig. 8). As a result the contribution above threshold starts at larger ω when increasing $\lambda(T)$.

3.3 Thermal width

The thermal width is given by

$$\Gamma_{\mathbf{p}} = -\frac{\text{Im}\Sigma_R(P)}{p^0} \Big|_{p^0=\pm\omega_{\mathbf{p}}} = -\frac{\text{Im}\Sigma_R(\omega_{\mathbf{p}}, \mathbf{p})}{\omega_{\mathbf{p}}}. \quad (68)$$

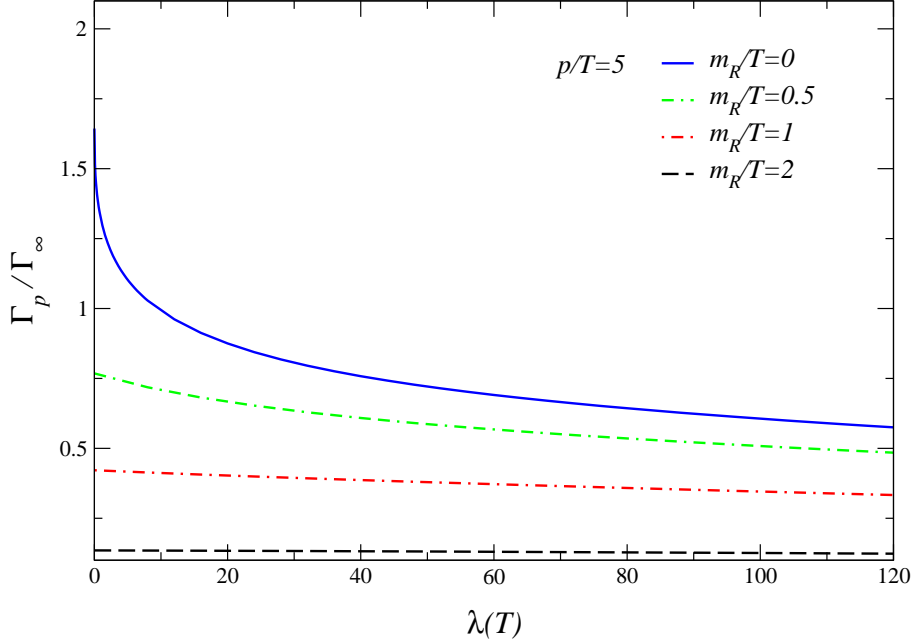


Figure 10: Width Γ_p/Γ_∞ as a function of $\lambda(T)$ for fixed $p/T = 5$ and four values of m_R/T .

The LO part of Σ does not contribute. We write the self energy at NLO as

$$\Sigma^{\text{NLO}}(P) = - \oint_R G(R) D(R - P). \quad (69)$$

After performing the Matsubara sum and the analytical continuation, we find $\text{Im}\Sigma_R$ in terms of spectral functions as

$$\text{Im}\Sigma_R(P) = \frac{1}{2} \int_R \rho(R) \rho_D(R - P) [n(r^0) - n(r^0 - p^0)]. \quad (70)$$

A convenient way to proceed is to introduce $k = |\mathbf{r} - \mathbf{p}|$ as

$$1 = \int_0^\infty dk \delta(k - |\mathbf{r} - \mathbf{p}|) = \int_{|r-p|}^{r+p} dk \frac{k}{rp} \delta(\cos \theta_{pr} - z_{pr}), \quad (71)$$

where $\cos \theta_{pr} = \hat{\mathbf{p}} \cdot \hat{\mathbf{r}}$ is the cosine of the angle between \mathbf{p} and \mathbf{r} and

$$z_{pr} = \frac{r^2 + p^2 - k^2}{2rp}. \quad (72)$$

We perform the r^0 integral using $\rho(R)$ and the θ_{pr} integral using the delta function introduced above. The final result for the width then reads

$$\Gamma_{\mathbf{p}} = \frac{1}{16\pi^2 p \omega_{\mathbf{p}}} \int_0^\infty dr \frac{r}{\omega_{\mathbf{r}}} \int_{|r-p|}^{r+p} dk k \left\{ \rho_D(\omega_{\mathbf{r}} + \omega_{\mathbf{p}}, k) [n(\omega_{\mathbf{r}}) - n(\omega_{\mathbf{r}} + \omega_{\mathbf{p}})] - \rho_D(\omega_{\mathbf{r}} - \omega_{\mathbf{p}}, k) [n(\omega_{\mathbf{r}}) - n(\omega_{\mathbf{r}} - \omega_{\mathbf{p}})] \right\}. \quad (73)$$

The remaining two integrals can be performed numerically. Note that to obtain ρ_D , a numerical evaluation of the real part of the bubble is required as well.

In Fig. 10 we show the width as a function of the coupling constant for fixed $p/T = 5$ and several choices of m_R/T . In order to remove the trivial parameter dependence, we rescaled $\Gamma_{\mathbf{p}}$ with

$$\Gamma_\infty = \frac{\lambda^2(M)T^2}{2403\pi N p}, \quad (74)$$

the thermal width at ultrahard momentum $p \gg T$ in the weakly coupled, massless limit at leading order in the $1/N$ expansion (see Sec. 6). We observe that for small mass the dependence on the coupling constant is substantial, whereas for larger mass it becomes negligible.

4 Shear viscosity

Now we have all the ingredients necessary to compute the shear viscosity. In order to do the Matsubara frequency sums, it is convenient to transform the integral equation for the 4-point function into an equivalent one for a 3-point vertex, defined in Fig. 11. The corresponding integral equation is depicted in Fig. 12. We denote the effective vertex as $\Gamma_{ij,ab}(P+Q, P)$ where P is the (euclidean) momentum on the siderails and $Q = (i\omega_q, \mathbf{0})$ the momentum that enters from the left. The integral equation then reads

$$\Gamma_{ij,ab}(P+Q, P) = \mathcal{D}_{ij,ab}^0(\mathbf{p}) + \frac{1}{2} \sum_R G(R+Q) \Gamma_{ij,cd}(R+Q, R) G(R) \Lambda_{cd;ab}(R, P; Q), \quad (75)$$

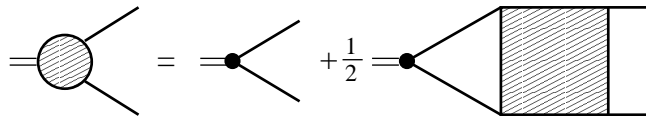


Figure 11: Relation between 3 and 4-point vertex function.

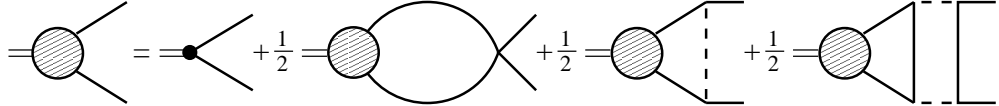


Figure 12: Integral equation for the full 3-point vertex.

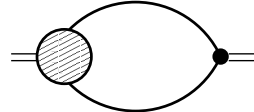


Figure 13: The correlator $\langle \pi_{ij} \pi_{ij} \rangle$ in terms of the full vertex.

where the kernel $\Lambda_{cd;ab}(R, P; Q)$ for vanishing Q was presented in Eqs. (30, 31) and the bare coupling between the scalar field and the π_{ij} operator follows from Eq. (5):

$$\mathcal{D}_{ij,ab}^0(\mathbf{p}) = 2\delta_{ab} \left[p_i p_j - \frac{1}{3} \delta_{ij} \mathbf{p}^2 \right]. \quad (76)$$

The correlator we need to obtain the shear viscosity takes the form of an effective one-loop diagram (see Fig. 13),

$$G_{\pi\pi}(Q) = \frac{1}{2} \not{\int}_P G(P+Q) \Gamma_{ij,ab}(P+Q, P) G(P) \mathcal{D}_{ij,ab}^0(\mathbf{p}). \quad (77)$$

The effective vertex can be taken of the form⁶

$$\Gamma_{ij,ab}(P+Q, P) = 2\delta_{ab} \left[p_i p_j - \frac{1}{3} \delta_{ij} \mathbf{p}^2 \right] \Gamma(P+Q, P), \quad (78)$$

which yields

$$G_{\pi\pi}(Q) = \frac{4}{3} N \not{\int}_P p^4 G(P+Q) \Gamma(P+Q, P) G(P). \quad (79)$$

In order to do the sums over the Matsubara frequencies, we follow the technique presented in Ref. [25], which makes use of the following relation

$$T \sum_n f(i\omega_n) = \sum_{\text{cuts}} \int_{-\infty}^{\infty} \frac{d\xi}{2\pi i} n(\xi) \text{Disc} f - \sum_{\text{poles}} n(z_i) \text{Res}(f, z_i), \quad (80)$$

⁶In principle, there could be an additional term proportional to δ_{ij} . However this would not contribute when contracted with the traceless bare vertex.

which requires knowledge of the analytical structure of the function to be summed. Because of the inclusion of the NLO contribution to the self energy in the propagators, the propagator $G(p^0, \mathbf{p})$ has a cut along the entire real p^0 axis, i.e. when $\text{Im}(p^0) = 0$ in the complex p^0 plane. It follows from the integral equation Eq. (75) that the effective vertex has the same analytic structure, namely, $\Gamma(P + Q, P)$ has cuts when $\text{Im}(p^0 + q^0) = 0$ and $\text{Im}(p^0) = 0$. With this information we can do the Matsubara frequency sum in Eq. (79), make the analytical continuation $i\omega_q \rightarrow q^0 + i0$ afterwards to arrive at the retarded function and take the limit $q^0 \rightarrow 0$ (see Refs. [25, 26] for further illustration). Only the product of retarded and advanced propagators suffers from pinching poles and dominates at leading order in the $1/N$ expansion. Therefore only one particular analytical continuation of the full vertex is needed. Defining

$$\mathcal{D}(p^0, \mathbf{p}) = \lim_{q^0 \rightarrow 0} \text{Re} \Gamma(p^0 + q^0 + i0, p^0 - i0; \mathbf{p}), \quad (81)$$

the result for the spectral density reads

$$\lim_{q^0 \rightarrow 0} \rho_{\pi\pi}(q^0, \mathbf{0}) = -\frac{8}{3} N q^0 \int_P p^4 n'(p^0) G_R(P) G_A(P) \mathcal{D}(p^0, \mathbf{p}). \quad (82)$$

Using Eq. (39) for the product of G_R and G_A and definition (3) for the shear viscosity, we get

$$\eta = -\frac{N}{15} \int_P n'(p^0) p^4 \frac{\rho(P)}{2p^0 \Gamma_{\mathbf{p}}} \mathcal{D}(p^0, \mathbf{p}) = -\frac{N}{15} \int_{\mathbf{p}} n'(\omega_{\mathbf{p}}) \frac{p^4}{\omega_{\mathbf{p}}^2} \frac{\mathcal{D}(p)}{\Gamma_{\mathbf{p}}}, \quad (83)$$

where we used that $n'(-\omega_{\mathbf{p}}) = n'(\omega_{\mathbf{p}})$ and we defined

$$\mathcal{D}(p) = \mathcal{D}(\pm\omega_{\mathbf{p}}, p). \quad (84)$$

To arrive at our final expression for the viscosity, we proceed as in the case of gauge theories [25, 26] and define the dimensionless quantity

$$\chi(p) = \frac{p^2}{\omega_{\mathbf{p}}} \frac{\mathcal{D}(p)}{\Gamma_{\mathbf{p}}}. \quad (85)$$

The shear viscosity then reads

$$\eta = -\frac{N}{15} \int_{\mathbf{p}} \frac{p^2}{\omega_{\mathbf{p}}} n'(\omega_{\mathbf{p}}) \chi(p) = -\frac{N}{30\pi^2} \int_0^\infty dp \frac{p^4}{\omega_{\mathbf{p}}} n'(\omega_{\mathbf{p}}) \chi(p). \quad (86)$$

Since the thermal width is inversely proportional to N , it follows that $\chi(p) \sim N$ in the large N limit.

5 Integral equation

As we have shown in the previous section, in order to obtain the shear viscosity, we need a particular analytic continuation of the effective vertex in the limit $q^0 \rightarrow 0$ and $p^0 = \pm \omega_{\mathbf{p}}$. In this section we first explicitly write down the integral equation in this kinematical limit. We then show how to cast it in a form suitable for a variational treatment. We also point out the relation between the integral equation and kinetic theory.

With momenta flowing as illustrated in Fig. 14, the integral equation reads

$$\Gamma_{ij,ab}(P+Q, P) = \mathcal{D}_{ij,ab}^0(\mathbf{p}) + \frac{1}{2} \sum_R G(R+Q) \Gamma_{ij,cd}(R+Q, R) G(R) \Lambda_{cd;ab}(R, P; Q), \quad (87)$$

where the rung is

$$\begin{aligned} \Lambda_{cd,ab}(R, P; Q) = & -\frac{\lambda_0}{3N} \delta_{ab} \delta_{cd} + (\delta_{ac} \delta_{bd} + \delta_{ad} \delta_{bc}) D(R - P) \\ & + 2 \delta_{ab} \delta_{cd} \sum_L D(L) D(L + Q) G(R - L) G(L - P). \end{aligned} \quad (88)$$

To arrive at a scalar equation we contract with $\mathcal{D}_{ij,ab}^0(\mathbf{p})$ and divide by a common factor to find

$$\Gamma(P+Q, P) = 1 + \frac{1}{2N} \sum_R \frac{r^2}{p^2} P_2(\hat{\mathbf{p}} \cdot \hat{\mathbf{r}}) G(R+Q) \Gamma(R+Q, R) G(R) \Lambda_{cc,aa}(R, P; Q). \quad (89)$$

Here, the second Legendre polynomial $P_2(x) = (3x^2 - 1)/2$ arises from the contraction

$$\mathcal{D}_{ij,ab}^0(\mathbf{p}) \Gamma_{ij,cd}(R+Q, R) = \frac{8}{3} p^2 r^2 P_2(\hat{\mathbf{p}} \cdot \hat{\mathbf{r}}) \delta_{ab} \delta_{cd} \Gamma(R+Q, R), \quad (90)$$

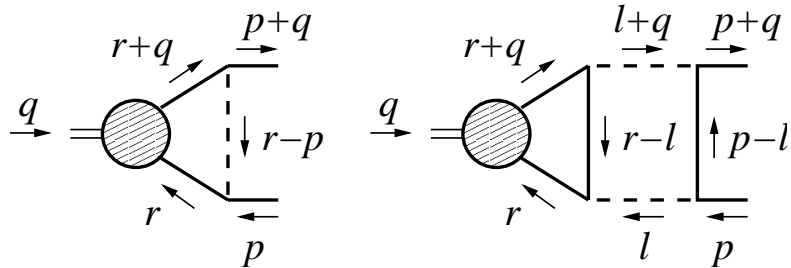


Figure 14: Choice of momentum labeling. We also denote $k = |\mathbf{r} - \mathbf{p}|$.

We now perform the Matsubara frequency sums following again the technique in Ref. [25]. The lowest order term in the rung does not contribute since it is a constant and it has no discontinuity. For doing the sum for the second term in the rung, we need to know that the auxiliary correlator $D(R - P)$ has a branch cut below the lightcone and above threshold (see Sec. 4.2). However, when using Eq. (80), we may assume that the cut runs along the entire real axis, since the contribution from where the cut is absent cancels automatically. Finally, for the last piece of the rung there are two sums. These can be performed sequentially, provided that the analytical continuation is made at the very end. The analytical structure is as follows. The G 's that depend on $R + Q$ and R as well as the vertex have branch cuts along the entire real energy axis, for the D 's we may take branch cuts along the entire real energy axis, and the G 's that depend on $R - L$ and $P - L$ contribute just simple poles (since they do not require the inclusion of the thermal width). When performing the sum over ω_l , one picks up contributions from the poles of the G 's and from the cuts of the D 's. We found that after making the analytical continuation only the poles from the G 's contribute.

From Eq. (81) it follows that we need the following analytic continuation

$$i\omega_p \rightarrow p^0 - i0, \quad i\omega_q \rightarrow q^0 + i0, \quad i\omega_p + i\omega_q \rightarrow p^0 + q^0 + i0, \quad (91)$$

Preserving again only the dominant contribution with pinching poles for vanishing q^0 , we arrive at

$$\mathcal{D}(P) = 1 + \int_R \frac{r^2}{p^2} P_2(\hat{\mathbf{p}} \cdot \hat{\mathbf{r}}) [n(r^0 - p^0) - n(r^0)] G_R(R) \mathcal{D}(R) G_A(R) \Lambda(R, P), \quad (92)$$

with

$$\Lambda(R, P) = \rho_D(R - P) + N \int_L [n(p^0 - l^0) - n(r^0 - l^0)] \rho(P - L) \rho(R - L) |D_R(L)|^2. \quad (93)$$

We note that the kernel obeys $\Lambda(R, P) = -\Lambda(P, R)$, $\Lambda(-R, P) = -\Lambda(R, -P)$.

We now use Eq. (39) for the product of G_R and G_A , Eqs. (84, 85) to introduce $\chi(p)$, and take $p^0 = \pm\omega_{\mathbf{p}}$ (both choices yield the same equation) to write the integral equation in the final form

$$\omega_{\mathbf{p}} \Gamma_{\mathbf{p}} \chi(p) = p^2 + \frac{1}{2} \int_R [n(r^0 - \omega_{\mathbf{p}}) - n(r^0)] \frac{\omega_{\mathbf{r}}}{r^0} P_2(\hat{\mathbf{p}} \cdot \hat{\mathbf{r}}) \chi(r) \rho(R) \Lambda(R, P). \quad (94)$$

Solving for $\chi(p)$, one obtains the shear viscosity from Eq. (86).

5.1 Variational approach

Since the integral equation cannot in general be solved analytically, one has to rely on numerical methods. A convenient approach to follow is the one employed in Refs. [19, 21, 22], where the problem of obtaining a transport coefficient in kinetic theory from an integral equation is formulated as a variational problem. Here we show how to cast the integral equation in a form that is suitable for a variational treatment.

After multiplying Eq. (94) with

$$\frac{p^2}{\omega_{\mathbf{p}}} n'(\omega_{\mathbf{p}}), \quad (95)$$

the integral equation can be written rather compactly as

$$\mathcal{F}(p)\chi(p) = \mathcal{S}(p) + \int_0^\infty dr \mathcal{H}(p, r)\chi(r), \quad (96)$$

with

$$\mathcal{F}(p) = p^2 n'(\omega_{\mathbf{p}}) \Gamma_{\mathbf{p}}, \quad \mathcal{S}(p) = \frac{p^4}{\omega_{\mathbf{p}}} n'(\omega_{\mathbf{p}}), \quad (97)$$

and a symmetric kernel

$$\mathcal{H}(p, r) = \mathcal{H}(r, p), \quad (98)$$

whose explicit form is presented below. Since \mathcal{H} is symmetric, Eq. (96) can be derived by extremizing the functional

$$Q[\chi] = \int_0^\infty dp \left[\mathcal{S}(p)\chi(p) - \frac{1}{2}\mathcal{F}(p)\chi^2(p) + \frac{1}{2} \int_0^\infty dr \mathcal{H}(p, r)\chi(r)\chi(p) \right]. \quad (99)$$

From Eq. (86) we see that the actual value of this functional at the extremum,

$$Q[\chi = \chi_{\text{ext}}] = \frac{1}{2} \int_0^\infty dp \mathcal{S}(p)\chi(p), \quad (100)$$

is directly proportional to the viscosity

$$\eta = -\frac{N}{15\pi^2} Q[\chi = \chi_{\text{ext}}]. \quad (101)$$

In the rest of this section we explicitly evaluate $\mathcal{H}(p, r)$.

We treat separately the diagram with the single line and with the box diagram and write $\mathcal{H} = \mathcal{H}_{\text{line}} + \mathcal{H}_{\text{box}}$. We start with the diagram containing the single line. The integral to evaluate reads

$$\int_R [n(r^0 - \omega_{\mathbf{p}}) - n(r^0)] \frac{\omega_{\mathbf{r}}}{r^0} P_2(\hat{\mathbf{p}} \cdot \hat{\mathbf{r}}) \chi(r) \rho(R) \rho_D(R - P). \quad (102)$$

We proceed in exactly the same way as in the case of the width in Sec. 3.3 and introduce $k = |\mathbf{r} - \mathbf{p}|$ via Eq. (71). We perform the r^0 integral using $\rho(R)$ and the integral over the angle between \mathbf{p} and \mathbf{r} using the delta function in Eq. (71). Multiplying the result with Eq. (95), we can immediately read the contribution to $\mathcal{H}(p, r)$ introduced above, and we find

$$\begin{aligned} \mathcal{H}_{\text{line}}(p, r) = \frac{n'(\omega_{\mathbf{p}})}{16\pi^2} \frac{p}{\omega_{\mathbf{p}}} \frac{r}{\omega_{\mathbf{r}}} \int_{|p-r|}^{p+r} dk k P_2(z_{pr}) \Big\{ & \rho_D(\omega_{\mathbf{r}} - \omega_{\mathbf{p}}, k) [n(\omega_{\mathbf{r}} - \omega_{\mathbf{p}}) - n(\omega_{\mathbf{r}})] \\ & - \rho_D(\omega_{\mathbf{r}} + \omega_{\mathbf{p}}, k) [n(\omega_{\mathbf{r}} + \omega_{\mathbf{p}}) - n(\omega_{\mathbf{r}})] \Big\}, \end{aligned} \quad (103)$$

where z_{pr} is given in Eq. (72). Using the relations

$$n(\omega_{\mathbf{r}} + \omega_{\mathbf{p}}) - n(\omega_{\mathbf{r}}) = \frac{Tn'(\omega_{\mathbf{r}})}{1 + n(\omega_{\mathbf{r}}) + n(\omega_{\mathbf{p}})}, \quad n(\omega_{\mathbf{r}} - \omega_{\mathbf{p}}) - n(\omega_{\mathbf{r}}) = \frac{Tn'(\omega_{\mathbf{r}})}{n(\omega_{\mathbf{r}}) - n(\omega_{\mathbf{p}})}, \quad (104)$$

and the fact that $\rho_D(\omega_{\mathbf{r}} - \omega_{\mathbf{p}}, k)$ is odd under interchange of p and r , it is straightforward to verify that the result is symmetric in p and r .

For the diagram containing the box rung, we have to evaluate

$$\begin{aligned} & \int_{R,L} [n(r^0 - \omega_{\mathbf{p}}) - n(r^0)] [n(\omega_{\mathbf{p}} - l^0) - n(r^0 - l^0)] \\ & \times P_2(\hat{\mathbf{p}} \cdot \hat{\mathbf{r}}) \chi(r) \frac{\omega_{\mathbf{r}}}{r^0} \rho(R) \rho(P - L) \rho(R - L) |D_R(L)|^2. \end{aligned} \quad (105)$$

There are three angular integrations that are nontrivial. We denote the cosine of the angle between \mathbf{p} and \mathbf{l} as $\cos \theta_{pl}$, between \mathbf{r} and \mathbf{l} as $\cos \theta_{rl}$, and the azimuthal angle between the \mathbf{p}, \mathbf{l} plane and the \mathbf{r}, \mathbf{l} plane as ϕ . The 8-dimensional integral can then be written as

$$\frac{2\pi}{(2\pi)^8} \int_0^\infty dr r^2 \int_{-\infty}^\infty dr^0 \int_0^\infty dl l^2 \int_{-\infty}^\infty dl^0 \int_{-1}^1 d\cos \theta_{pl} \int_{-1}^1 d\cos \theta_{rl} \int_0^{2\pi} d\phi. \quad (106)$$

The integration over $\cos \theta_{pl}$ will be performed using the delta functions in $\rho(P - L)$, the one over $\cos \theta_{rl}$ using $\rho(R - L)$ and that over r^0 using $\rho(R)$. The product of the

three spectral functions yields a set of constraints, since

$$\begin{aligned} \rho(R)\rho(P-L)\rho(R-L)\Big|_{p^0=\omega_{\mathbf{p}}} &\sim \sum_{s_i=\pm} \delta(r^0 + s_1\omega_{\mathbf{r}})\delta(\omega_{\mathbf{p}} - l^0 + s_2\omega_{\mathbf{p}-\mathbf{l}})\delta(r^0 - l^0 - s_3\omega_{\mathbf{r}-\mathbf{l}}) \\ &\sim \sum_{s_i=\pm} \delta(\omega_{\mathbf{p}} + s_1\omega_{\mathbf{r}} + s_2\omega_{\mathbf{p}-\mathbf{l}} + s_3\omega_{\mathbf{r}-\mathbf{l}}). \end{aligned} \quad (107)$$

Out of the eight combinations, only three can contribute for kinematical reasons, namely those corresponding to $2 \leftrightarrow 2$ processes. We treat these three cases separately and write

$$\mathcal{H}_{\text{box}} = \mathcal{H}_{\text{box}}^{(1)} + \mathcal{H}_{\text{box}}^{(2)} + \mathcal{H}_{\text{box}}^{(3)}. \quad (108)$$

1. $(s_1, s_2, s_3) = (-, +, -)$. The cosines are $\cos\theta_{pl} = z_{pl}$, $\cos\theta_{rl} = z_{rl}^-$, where

$$z_{pl} = \frac{l^2 - l_0^2}{2pl} + \frac{\omega_{\mathbf{p}}l^0}{pl}, \quad z_{rl}^{s_1} = \frac{l^2 - l_0^2}{2rl} - s_1 \frac{\omega_{\mathbf{r}}l^0}{rl}. \quad (109)$$

The constraints from the spectral functions can be satisfied provided

$$l^0 > \sqrt{l^2 + 4M^2}, \quad |l_-| < p, r < |l_+|, \quad (110)$$

where here and below

$$l_{\pm} = \frac{1}{2} [l \pm l^0 \beta(L)], \quad \beta(L) = \sqrt{1 - \frac{4M^2}{l_0^2 - l^2}}. \quad (111)$$

The only place where the angle ϕ appears is in $\hat{\mathbf{p}} \cdot \hat{\mathbf{r}}$, which when expressed in terms of the angles we use, reads

$$\hat{\mathbf{p}} \cdot \hat{\mathbf{r}} = \sin\theta_{pl} \sin\theta_{rl} \cos\phi + \cos\theta_{pl} \cos\theta_{rl}. \quad (112)$$

It is then also straightforward to perform the ϕ -integral and we find

$$\int_0^{2\pi} d\phi P_2(\hat{\mathbf{p}} \cdot \hat{\mathbf{r}}) = 2\pi P_2(\cos\theta_{pl})P_2(\cos\theta_{rl}). \quad (113)$$

Multiplying the resulting expression with Eq. (95) we can read off the first contribution to $\mathcal{H}(p, r)$ from the box diagram:

$$\begin{aligned} \mathcal{H}_{\text{box}}^{(1)}(p, r) &= \frac{N}{128\pi^3} \frac{p}{\omega_{\mathbf{p}}} \frac{r}{\omega_{\mathbf{r}}} n'(\omega_{\mathbf{p}}) [n(\omega_{\mathbf{r}} - \omega_{\mathbf{p}}) - n(\omega_{\mathbf{r}})] \\ &\times \int_0^{\infty} dl \int_{\sqrt{l^2+4M^2}}^{\infty} dl^0 P_2(z_{pl})P_2(z_{rl}^-) |D_R(L)|^2 [n(\omega_{\mathbf{p}} - l^0) - n(\omega_{\mathbf{r}} - l^0)] \\ &\times \Theta(p - |l_-|) \Theta(|l_+| - p) \Theta(r - |l_-|) \Theta(|l_+| - r). \end{aligned} \quad (114)$$

2. $(s_1, s_2, s_3) = (-, -, +)$. The cosines are $\cos \theta_{pl} = z_{pl}$, $\cos \theta_{rl} = z_{rl}^-$ and the constraints are

$$l_0^2 < l^2, \quad p > |l_+|, \quad r > |l_+|. \quad (115)$$

Therefore the second contribution reads

$$\begin{aligned} \mathcal{H}_{\text{box}}^{(2)}(p, r) &= \frac{N}{128\pi^3} \frac{p}{\omega_p} \frac{r}{\omega_r} n'(\omega_p) [n(\omega_r - \omega_p) - n(\omega_r)] \\ &\times \int_0^\infty dl \int_{-l}^l dl^0 P_2(z_{pl}) P_2(z_{rl}^-) |D_R(L)|^2 [n(\omega_p - l^0) - n(\omega_r - l^0)] \\ &\times \Theta(p - |l_+|) \Theta(r - |l_+|). \end{aligned} \quad (116)$$

3. $(s_1, s_2, s_3) = (+, -, -)$. In this case the cosines are $\cos \theta_{pl} = z_{pl}$, $\cos \theta_{rl} = z_{rl}^+$, with the constraints

$$l_0^2 < l^2, \quad p > |l_+|, \quad r > |l_-|. \quad (117)$$

The third contribution then reads

$$\begin{aligned} \mathcal{H}_{\text{box}}^{(3)}(p, r) &= \frac{N}{128\pi^3} \frac{p}{\omega_p} \frac{r}{\omega_r} n'(\omega_p) [n(\omega_r + \omega_p) - n(\omega_r)] \\ &\times \int_0^\infty dl \int_{-l}^l dl^0 P_2(z_{pl}) P_2(z_{rl}^+) |D_R(L)|^2 [n(l^0 - \omega_p) - n(l^0 + \omega_r)] \\ &\times \Theta(p - |l_+|) \Theta(r - |l_-|). \end{aligned} \quad (118)$$

Using relations (104) and making the substitution $l^0 \rightarrow -l^0$ in the third contribution, one finds that $\mathcal{H}_{\text{box}}(p, r) = \mathcal{H}_{\text{box}}(r, p)$. In conclusion, $\mathcal{H}(p, r) = \mathcal{H}(r, p)$, which allows to obtain the integral equation from the functional Q .

5.2 Kinetic theory

Here we briefly mention the relation between our results and the corresponding kinetic theory, by analyzing the kernel in the integral equation.

The kernel $\Lambda(R, P)$ can be written in a form that allows for a direct comparison with kinetic theory. We start by changing variables $L \rightarrow P - L$ and find

$$\Lambda(R, P) = \rho_D(R - P) + N \int_L \left[n(l^0) - n(r^0 - p^0 + l^0) \right] \rho(L) \rho(R - P + L) |D_R(P - L)|^2. \quad (119)$$

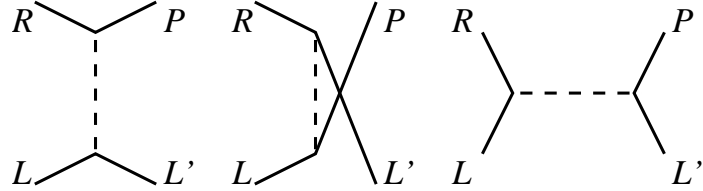


Figure 15: Scattering processes in kinetic theory, time runs horizontally.

If we use for the spectral density the following identity

$$\rho_D(R - P) = -2\text{Im}\Pi_R(R - P) |D_R(R - P)|^2, \quad (120)$$

where (see Eq. (62))

$$\text{Im}\Pi_R(R - P) = -\frac{N}{4} \int_L [n(l^0) - n(r^0 - p^0 + l^0)] \rho(L) \rho(R - P + L), \quad (121)$$

introduce the variable L' according to

$$\int_{L'} (2\pi)^4 \delta^4(R - P + L - L') \quad (122)$$

and use the delta function to interchange momentum labels, the kernel can be written as

$$\begin{aligned} \Lambda(R, P) &= \frac{N}{2} \int_{L, L'} [n(l^0) - n(l'^0)] \rho(L) \rho(L') (2\pi)^4 \delta^4(R - P + L - L') \\ &\times \left[|D_R(R - P)|^2 + |D_R(R - L')|^2 + |D_R(R + L)|^2 \right]. \end{aligned} \quad (123)$$

The second line is precisely the sum of the squares of the matrix elements $|\mathcal{M}|^2$ for scattering $(R, L) \rightarrow (P, L')$ in kinetic theory, where the auxiliary correlator carries the interaction (see Fig. 15). There are no interference terms (these would appear from the square of the sum of matrix elements): interference only contributes at the next order in the $1/N$ expansion.

6 Weak coupling

In the limit of weak coupling, the integral equation simplifies considerably and it is possible to obtain an approximate analytical solution. At weak coupling, we make

the replacements

$$D_{R/A}(P) \rightarrow -\frac{\lambda}{3N}, \quad \rho_D(P) \rightarrow -\left(\frac{\lambda}{3N}\right)^2 2\text{Im}\Pi_R(P), \quad (124)$$

so that the kernel becomes

$$\Lambda(R, P) \rightarrow -6\left(\frac{\lambda}{3N}\right)^2 \text{Im}\Pi_R(R - P), \quad (125)$$

and the width reads

$$\Gamma_{\mathbf{p}} = \frac{1}{\omega_{\mathbf{p}}} \left(\frac{\lambda}{3N}\right)^2 \int_R \rho(R) \text{Im}\Pi_R(R - P) [n(r^0) - n(r^0 - \omega_{\mathbf{p}})]. \quad (126)$$

We will use the integral equation in the form

$$\omega_{\mathbf{p}} \Gamma_{\mathbf{p}} \chi(p) = p^2 + \frac{1}{2} \int_R [n(r^0 - \omega_{\mathbf{p}}) - n(r^0)] \frac{\omega_{\mathbf{r}}}{r^0} P_2(\hat{\mathbf{p}} \cdot \hat{\mathbf{r}}) \chi(r) \rho(R) \Lambda(R, P). \quad (127)$$

Both on the left and the right-hand side of this equation two integrals (over r and $k = |\mathbf{r} - \mathbf{p}|$) remain to be done. The imaginary part of the single bubble $\text{Im}\Pi_R$ is known analytically, see Eq. (64). For this reason the weakly coupled case is considerably easier than the full problem.

For the massless weakly coupled theory, we will now show that it is possible to find an approximate analytical solution in the limit $p \rightarrow \infty$. Consider first the thermal width on the LHS. Evaluating the two remaining integrals in that limit one finds (see also Appendix G in Ref. [23] for the case $N = 1$)

$$\lim_{p \rightarrow \infty} \Gamma_{\mathbf{p}} = \frac{1}{2304\pi} \frac{\lambda^2 T^2}{pN} \left[1 + \frac{24\zeta(3)}{\pi^2} \frac{T}{p} + \mathcal{O}(e^{-p/T}) \right]. \quad (128)$$

Neglecting for a moment the ladder contribution on the RHS of the integral equation, it is easy to solve for $\chi(p)$ and we find

$$\lim_{p \rightarrow \infty} \chi(p) = 2304\pi \frac{N}{\lambda^2} \frac{p^2}{T^2} [1 + \mathcal{O}(T/p)]. \quad (\text{no ladders}). \quad (129)$$

To include the ladders we now use the same momentum dependence for χ but with an arbitrary prefactor

$$\chi(p) = \kappa p^2. \quad (130)$$

Inserting this ansatz on the RHS of the integral, performing the integrals while consistently dropping terms that are suppressed with respect to the leading p^2 behavior, we find the following result for the complete integral equation:

$$\frac{\lambda^2 T^2}{2304\pi N} \kappa p^2 [1 + \mathcal{O}(T/p)] = p^2 + \frac{\lambda^2 T^2}{3456\pi N} \kappa p^2 [1 + \mathcal{O}(T/p)]. \quad (131)$$

The solution for ultrahard p is therefore

$$\lim_{p \rightarrow \infty} \chi(p) = 6912\pi \frac{N}{\lambda^2} \frac{p^2}{T^2}. \quad (132)$$

A comparison between the asymptotic solution without ladders, Eq. (129), and with ladders, Eq. (132), reveals that the effect of summing ladders is simply algebraic: the full vertex $\mathcal{D}(p)$ in Eq. (85) equals 3.

Using this asymptotic form of $\chi(p)$ in expression (86) for the viscosity yields

$$\eta_\infty = \frac{27648\zeta(5)}{\pi} \frac{N^2 T^3}{\lambda^2} \approx 9125.6 \frac{N^2 T^3}{\lambda^2}, \quad (133)$$

where the subscript indicates that this solution has been obtained for ultrahard momentum p .

We can compare this result with the numerical results obtained for the shear viscosity in Refs. [23, 19] for the weakly coupled massless $N = 1$ theory. In order to do this we must find the full N dependence at weak coupling, not just the leading order result $\propto N^2$. For this we use again the 2PI effective action, but now employing the loop expansion to three loops. The important formulas are summarized in Appendix A. The result is that the full N dependence of the shear viscosity is quite simple, and we find

$$\eta_\infty = \frac{27648\zeta(5)}{\pi} \frac{N^3}{N+2} \frac{T^3}{\lambda^2} \approx 3041.9 \frac{3N^3}{N+2} \frac{T^3}{\lambda^2}. \quad (134)$$

The numerical constant is extremely close to the ones obtained numerically in Ref. [23] (3040) and Ref. [19] (3033.5).

7 Variational solution

In order to obtain the shear viscosity for general values of the coupling constant and mass parameter, we solve the problem of extremizing the functional Q in Eq. (99)

variationally. Following Arnold, Moore and Yaffe [19, 21, 22], we expand $\chi(p)$ in a finite set of suitably chosen basis functions $\phi^{(m)}(p)$:

$$\chi(p) = N \sum_{m=1}^{N_{\text{var}}} a_m \phi^{(m)}(p), \quad (135)$$

where we factored out an explicit factor of N , so that the integrals below are N -independent. Using this Ansatz in the functional Q yields

$$Q[\chi] = N \sum_m a_m \left[\mathcal{S}_m + \frac{1}{2} \sum_n a_n (-\mathcal{F}_{mn} + \mathcal{H}_{mn}) \right], \quad (136)$$

with

$$\begin{aligned} \mathcal{S}_m &= \int_0^\infty dp \mathcal{S}(p) \phi^{(m)}(p), \\ \mathcal{F}_{mn} &= N \int_0^\infty dp \mathcal{F}(p) \phi^{(m)}(p) \phi^{(n)}(p), \\ \mathcal{H}_{mn} &= N \int_0^\infty dp \int_0^\infty dr \mathcal{H}(p, r) \phi^{(m)}(p) \phi^{(n)}(r). \end{aligned} \quad (137)$$

Note that \mathcal{S}_m is a 1-dimensional integral, \mathcal{F}_{mn} and \mathcal{H}_{mn} for the line diagram are 3-dimensional integrals, and \mathcal{H}_{mn} for the box diagram is a 4-dimensional integral. Extremizing the functional with respect to the variational parameters a_m gives a simple linear algebra problem. The shear viscosity is given by

$$\eta = -\frac{N^2}{30\pi^2} \sum_m \mathcal{S}_m a_m, \quad a_m = \sum_n (\mathcal{F} - \mathcal{H})_{mn}^{-1} \mathcal{S}_n. \quad (138)$$

Given the asymptotic solution $\chi(p) \sim (p/T)^2$, our choice for the trial functions is

$$\phi^{(m)}(p) = \frac{(p/T)^2}{(1+p/T)^{m-1}} \sum_{k=0}^{m-1} (-1)^k (p/T)^k. \quad (139)$$

For fixed N_{var} these basis functions are a linear combination of the functions used in Refs. [19, 21, 22]. For given basis functions the integrals in Eq. (137) can now be performed numerically. We found that the presence of the mass M in the integration boundaries for p and r in \mathcal{H}_{box} (see Sec. 5.2) reduces the effort required for the numerical integration compared to the massless case. Using straightforward quadrature,

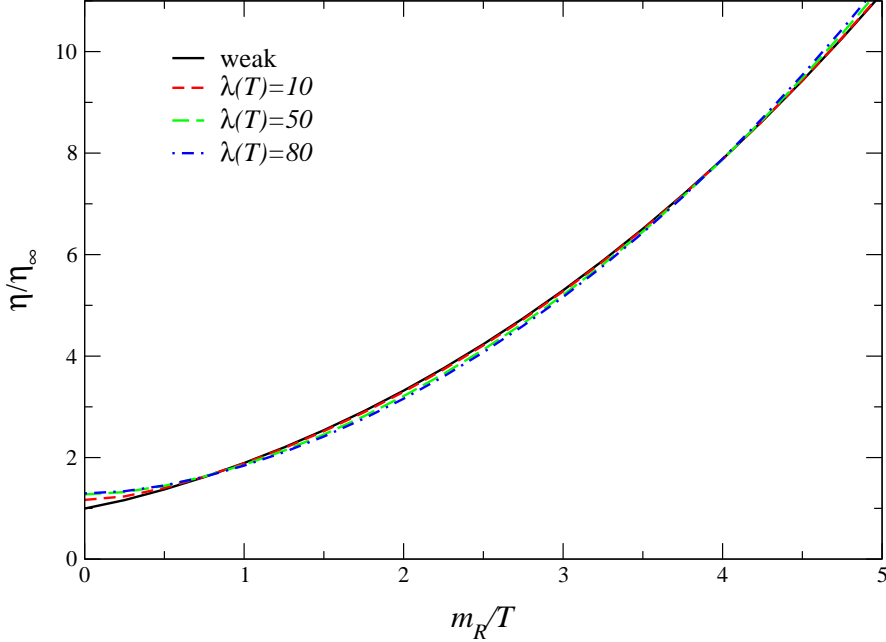


Figure 16: Shear viscosity η/η_∞ as a function of m_R/T , for four values of $\lambda(\mu = T)$. Weak denotes the result in the limit $\lambda \rightarrow 0$, i.e. keeping only the single bubble in the rung.

the errors due to the numerical integration are smaller than the width of the lines in Figs. 16, 17. Also, the results shown in these figures are obtained using three basis functions. Again, the effect of using this truncated basis set is smaller than the width of the lines.

In Fig. 16 we present the shear viscosity as a function of the renormalized mass in vacuum. To remove the trivial $N^2 T^3 / \lambda^2$ dependence, we scaled the result with the approximate analytical solution η_∞ (see Eq. (133)). The line labeled ‘weak’ shows the result in the weak coupling limit $\lambda \rightarrow 0$, i.e. preserving only the single bubble in the rung. The other lines represent the solution to the full problem for various values of $\lambda(T)$. We have chosen $\mu = T$ to present our results, but the shear viscosity is RG invariant. We observe that the shear viscosity has a characteristic dependence on the mass, but a negligible dependence on the coupling constant, after the dominant $1/\lambda^2$ behavior has been scaled out.

In order to analyze this in more detail, we show in Fig. 17 the shear viscosity as a function of the coupling constant $\lambda(T)$ for various values of the renormalized mass at zero temperature. Recall that because of the scaling with η_∞ , we concentrate here on

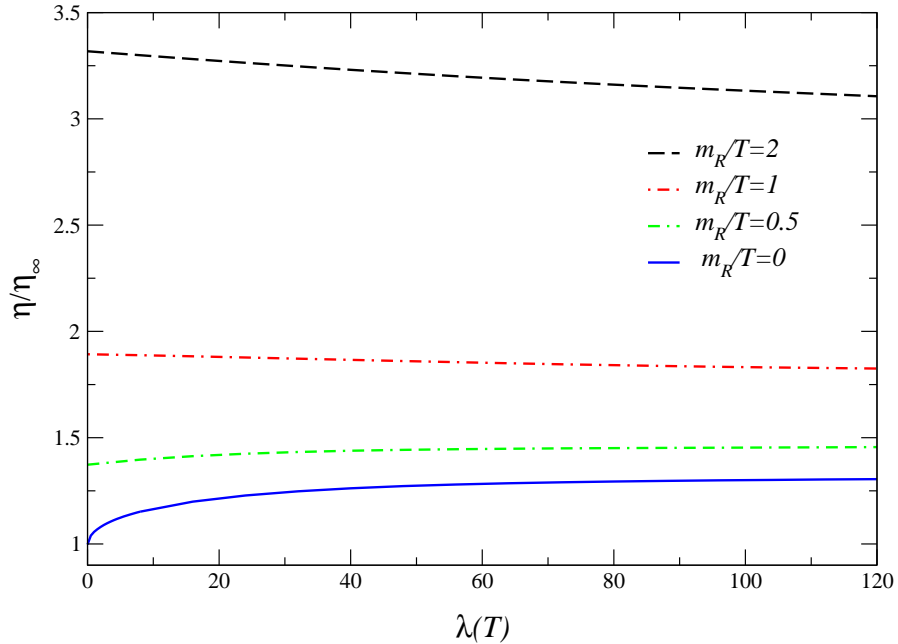


Figure 17: Shear viscosity η/η_∞ as a function of $\lambda(\mu = T)$, for 4 different values of m_R/T .

the subdominant λ dependence. We find an appreciable dependence on the coupling constant only for vanishing mass. Comparison with the thermal width in Fig. 10 shows that for small m_R , the shear viscosity and the inverse width have a similar dependence on the coupling constant, as expected.

8 Conclusions

We have presented a diagrammatic calculation of the shear viscosity in the $O(N)$ model at first nontrivial order in the large N limit. The $1/N$ expansion of the 2PI effective action at next-to-leading order leads in a straightforward manner to the diagrams contributing to the shear viscosity at leading order and provides automatically the integral equation required to sum them.

In the weakly coupled massless theory, the integral equation could be analyzed analytically in the limit of ultrahard momentum. Using this result we found for the

shear viscosity in the $O(N)$ model

$$\eta_\infty = \frac{9216\zeta(5)}{\pi} \frac{3N^3}{N+2} \frac{T^3}{\lambda^2} \approx 3041.9 \frac{3N^3}{N+2} \frac{T^3}{\lambda^2}. \quad (140)$$

This result is extremely close to the numerical values determined earlier for the single component theory ($N = 1$).

For the general case we computed the shear viscosity numerically through a variational approach. The results are presented in Figs. 16 and 17. Factoring out the basic $1/\lambda^2$ dependence, the results show that the remaining dependence on the coupling constant is very weak, while the effect on the mass parameter is larger. For the allowed range of parameters, we conclude that the shear viscosity is close to the result obtained in the weak-coupling analysis.

From a more general point of view, we found that the availability of an effective action that sums the appropriate diagrams is extremely useful. While the computation of transport coefficients is still quite involved, it is streamlined by the organization inherent in the 2PI effective action. From the wider perspective of nonequilibrium quantum fields, it is satisfying that 2PI effective action techniques can be applied both far from equilibrium, relying mostly on numerical tools, as well as (very) close to equilibrium, as we have demonstrated here.

As we have argued recently [14], the first nontrivial truncation of the 2PI effective action also sums the relevant diagrams to obtain the shear viscosity and the electrical conductivity in gauge theories to leading-logarithmic order in the weak coupling limit or to leading order in a $1/N_f$ expansion, where N_f is the number of fermion fields. A diagrammatic analysis of transport coefficients in gauge theories beyond the leading-log approximation at weak coupling is not yet available. A convenient starting point for such an analysis may be based on a more general n PI effective action approach [39].

Acknowledgments. Discussions with U. Heinz are gratefully acknowledged. This research was supported in part by the U. S. Department of Energy under Contract No. DE-FG02-01ER41190 and No. DE-FG02-91-ER4069 and by the Basque Government and in part by the Spanish Science Ministry (Grant FPA 2002-02037) and the University of the Basque Country (Grant UPV00172.310-14497/2002).

A Three-loop expansion

In order to find the full N dependence of the shear viscosity in the $O(N)$ model in the weak coupling limit and not just its leading behavior at large N , we summarize

here the results for the three-loop expansion of the 2PI effective action. We write $\Gamma_2[G] = \sum_{l=2}^{\infty} \Gamma_2^{(l)}[G]$, with

$$\Gamma_2^{(2)}[G] = -\frac{\lambda}{8} \frac{N+2}{3} \int_x G^2(x, x), \quad (141)$$

$$\Gamma_2^{(3)}[G] = \frac{i\lambda^2}{48} \frac{N+2}{3N} \int_{xy} G^4(x, y). \quad (142)$$

Since mass and coupling constant renormalization do not enter here, we denote the coupling constant with λ . We also immediately specialized to $G_{ab} = \delta_{ab}G$. The corresponding self energies are

$$\Sigma_{ab}^{(2)}(x, y) = -i \frac{\lambda}{2} \frac{N+2}{3N} \delta_{ab} G(x, x) \delta_C(x - y), \quad (143)$$

$$\Sigma_{ab}^{(3)}(x, y) = -\frac{\lambda^2}{6} \frac{N+2}{3N^2} \delta_{ab} G^3(x, y), \quad (144)$$

and the kernel reads

$$\begin{aligned} \Lambda_{ab;cd}^{(2)}(x, y; x', y') &= -i \frac{\lambda}{3N} [\delta_{ab}\delta_{cd} + \delta_{ac}\delta_{bd} + \delta_{ad}\delta_{bc}] \\ &\quad \times \delta_C(x - y) \delta_C(x - y') \delta_C(x' - y), \end{aligned} \quad (145)$$

$$\begin{aligned} \Lambda_{ab;cd}^{(3)}(x, y; x', y') &= -\frac{\lambda^2}{18N^2} [4\delta_{ab}\delta_{cd} + (N+6)(\delta_{ac}\delta_{bd} + \delta_{ad}\delta_{bc})] \\ &\quad \times G^2(x, y) \delta_C(x - x') \delta_C(y - y'). \end{aligned} \quad (146)$$

In particular we find that

$$\Lambda_{aa;cc}^{(3)}(x, y; x', y') = -\lambda^2 \frac{N+2}{3N} G^2(x, y) \delta_C(x - x') \delta_C(y - y'). \quad (147)$$

Using these expressions it is straightforward to find the N dependence of the shear viscosity in the $O(N)$ model for arbitrary N . Starting from the large N result in the weak coupling limit, the thermal width $\Gamma_{\mathbf{p}}$ and the kernel Λ are related to the thermal width and the kernel presented in Sec. 6 as

$$\Gamma_{\mathbf{p}} \Big|_{\text{arbitrary } N} = \frac{N+2}{N} \Gamma_{\mathbf{p}} \Big|_{\text{large } N}, \quad (148)$$

$$\Lambda(R, P) \Big|_{\text{arbitrary } N} = \frac{N+2}{N} \Lambda(R, P) \Big|_{\text{large } N}. \quad (149)$$

The N dependence that subsequently appears in the integral equation can be absorbed in $\chi(p)$ as

$$\chi(p) \Big|_{\text{arbitrary } N} = \frac{N}{N+2} \chi(p) \Big|_{\text{large } N}, \quad (150)$$

so the final effect in the viscosity is quite simple:

$$\eta \Big|_{\text{arbitrary } N} = \frac{N}{N+2} \eta \Big|_{\text{large } N}. \quad (151)$$

In the weakly coupled massless limit we arrive therefore at the analytical result,

$$\eta_\infty = \frac{9216\zeta(5)}{\pi} \frac{3N^3}{N+2} \frac{T^3}{\lambda^2}, \quad (152)$$

for the shear viscosity in the $O(N)$ model.

References

- [1] J. Berges and J. Cox, Phys. Lett. B **517**, 369 (2001) [hep-ph/0006160].
- [2] B. Mihaila, F. Cooper and J. F. Dawson, Phys. Rev. D **63**, 096003 (2001) [hep-ph/0006254]; *ibid.* **67** (2003) 051901 [hep-ph/0207346]; *ibid.* **67** (2003) 056003 [hep-ph/0209051].
- [3] G. Aarts and J. Berges, Phys. Rev. D **64**, 105010 (2001) [hep-ph/0103049].
- [4] J. Berges, Nucl. Phys. A **699**, 847 (2002) [hep-ph/0105311].
- [5] G. Aarts and J. Berges, Phys. Rev. Lett. **88**, 041603 (2002) [hep-ph/0107129].
- [6] G. Aarts, D. Ahrensmeier, R. Baier, J. Berges and J. Serreau, Phys. Rev. D **66**, 045008 (2002) [hep-ph/0201308].
- [7] J. Berges and J. Serreau, Phys. Rev. Lett. **91** (2003) 111601 [hep-ph/0208070].
- [8] J. Berges, S. Borsányi and J. Serreau, Nucl. Phys. B **660** (2003) 51 [hep-ph/0212404].
- [9] B. Mihaila, Phys. Rev. D **68**, 036002 (2003) [hep-ph/0303157].
- [10] E. A. Calzetta and B. L. Hu, Phys. Rev. D **68**, 065027 (2003) [hep-ph/0305326].

- [11] S. Juchem, W. Cassing and C. Greiner, Phys. Rev. D **69** (2004) 025006 [hep-ph/0307353]; nucl-th/0401046.
- [12] D. J. Bedingham, hep-ph/0310133.
- [13] T. Ikeda, hep-ph/0401045.
- [14] G. Aarts and J. M. Martínez Resco, Phys. Rev. D **68** (2003) 085009 [hep-ph/0303216].
- [15] E. A. Calzetta, B. L. Hu and S. A. Ramsey, Phys. Rev. D **61**, 125013 (2000) [hep-ph/9910334].
- [16] J. Baacke and A. Heinen, Phys. Rev. D **67** (2003) 105020 [hep-ph/0212312]; *ibid.* **68** (2003) 127702 [hep-ph/0305220].
- [17] For a review, see e.g. P. F. Kolb and U. Heinz, to appear in “Quark Gluon Plasma 3,” nucl-th/0305084.
- [18] D. Teaney, Phys. Rev. C **68** (2003) 034913 [nucl-th/0301099].
- [19] P. Arnold, G. D. Moore and L. G. Yaffe, JHEP **0011**, 001 (2000) [hep-ph/0010177].
- [20] P. Arnold, G. D. Moore and L. G. Yaffe, JHEP **0301**, 030 (2003) [hep-ph/0209353].
- [21] P. Arnold, G. D. Moore and L. G. Yaffe, JHEP **0305** (2003) 051 [hep-ph/0302165].
- [22] G. D. Moore, JHEP **0105**, 039 (2001) [hep-ph/0104121].
- [23] S. Jeon, Phys. Rev. D **52**, 3591 (1995) [hep-ph/9409250].
- [24] E. Wang and U. Heinz, Phys. Rev. D **67**, 025022 (2003) [hep-th/0201116].
- [25] M. A. Valle Basagoiti, Phys. Rev. D **66**, 045005 (2002) [hep-ph/0204334].
- [26] G. Aarts and J. M. Martínez Resco, JHEP **0211**, 022 (2002) [hep-ph/0209048].
- [27] D. Boyanovsky, H. J. de Vega and S. Y. Wang, Phys. Rev. D **67** (2003) 065022 [hep-ph/0212107].

- [28] G. Aarts and J. M. Martínez Resco, JHEP **0204** (2002) 053 [hep-ph/0203177]; Nucl. Phys. Proc. Suppl. **119** (2003) 505 [hep-lat/0209033].
- [29] S. Gupta, hep-lat/0301006.
- [30] For earlier attempts, see F. Karsch and H. W. Wyld, Phys. Rev. D **35** (1987) 2518; S. Sakai, A. Nakamura and T. Saito, Nucl. Phys. Proc. Suppl. **106** (2002) 543 [hep-lat/0110177].
- [31] G. Policastro, D. T. Son and A. O. Starinets, Phys. Rev. Lett. **87** (2001) 081601 [hep-th/0104066]; JHEP **0209** (2002) 043 [hep-th/0205052].
- [32] A. Muronga, nucl-th/0309056.
- [33] A. Dobado and F. J. Llanes-Estrada, hep-ph/0309324.
- [34] J. M. Cornwall, R. Jackiw and E. Tomboulis, Phys. Rev. D **10** (1974) 2428.
- [35] See also J.M. Luttinger and J.C. Ward, Phys. Rev. **118** (1960) 1417; G. Baym, Phys. Rev. **127** (1962) 1391.
- [36] P. Kovtun, D. T. Son and A. O. Starinets, JHEP **0310** (2003) 064 [hep-th/0309213].
- [37] H. van Hees and J. Knoll, Phys. Rev. D **65**, 025010 (2002) [hep-ph/0107200]; *ibid.* 105005 (2002) [hep-ph/0111193].
- [38] J. P. Blaizot, E. Iancu and U. Reinosa, Phys. Lett. B **568** (2003) 160 [hep-ph/0301201]; hep-ph/0312085.
- [39] J. Berges, hep-ph/0401172.